JMEPEG (2012) 21:2719–2728
DOI: 10.1007/s11665-012-0414-x
©ASM International
1059-9495/$19.00

Experimental Evaluation of a Device Prototype Based on Shape Memory Alloys for the Retrofit of Historical Buildings

Donatello Cardone and Salvatore Sofia

(Submitted March 14, 2012; in revised form October 2, 2012)

Metallic tie-rods are currently used in many historical buildings for absorbing the out-of-plane horizontal forces of arches, vaults and roof trusses, despite they exhibit several limitations under service and seismic conditions. In this paper, a post-tensioned system based on the superelastic properties of Ni-Ti shape memory alloys is proposed for improving the structural performances of traditional metallic tie-rods. First, the thermal behavior under service conditions is investigated based on the results of numerical and experimental studies. Subsequently, the seismic performances under strong earthquakes are verified trough a number of shaking table tests on a 1:4-scale timber roof truss model. The outcomes of these studies fully confirm the achievement of the design objectives of the proposed prototype device.

Keywords air temperature variations, historical buildings, seismic response, shaking table tests, shape memory alloys

1. Introduction

Degradation of ancient building materials, prolonged exposure to environmental influences and uneven settlements make strengthening of historic buildings unavoidable. Furthermore, many historic buildings were built to a much lower seismic intensity compared to similar modern structures. Seismic retrofit measures, integrated into the building without altering its character and appearance, are then needed. Arches, vaults, and timber roof trusses are typical elements of historic buildings. In many cases, however, proper structural details for absorbing the out-of-plane horizontal thrusts exerted by these typical elements (e.g., concrete curbs, wood tie beams, steel tie-rods) are missing, inadequate, or deteriorated.

In the last decades, some researchers have started proposing SMA as kernel components of passive control devices for improving the dynamic response of buildings and bridges subjected to earthquake-induced vibrations (Ref 1-12).

In this paper, a post-tensioned system based on the superelastic properties of shape memory alloys (SMAs) is presented as an alternative to currently used metallic tie-rods.

The main advantage of the proposed SMA-based system, compared to traditional metallic tie-rods, is the possibility of limiting force changes in the latter due to temperature variations. Additional features are related to the possibility of: (i) calibrating the stress in the system during the post-tensioned process, (ii) avoiding buckling under negative displacements, (iii) applying the force in the anchorages without jerks during an earthquake, (iv) controlling the structural deformations, if a given target displacement is exceeded, under unexpected earthquakes, (v) dissipating a significant amount of energy during an earthquake.

First, the thermal behavior under service conditions of a steel tie-rod, with and without SMA device, is evaluated. To this end, a suitable iterative numerical procedure, able to simulate the interaction between steel tie-rod and SMA device under a given temperature-time history, has been implemented and applied to a selected case study, in order to demonstrate the improvements following the use of the SMA unit. The seismic effectiveness of the proposed SMA system is then verified through a number of shaking table tests on a 1:4-scale timber roof truss model equipped with a suitable SMA unit. The comparison between the seismic response of the structure, with and without the SMA unit, fully confirms the achievement of the design objectives.

2. Performance Objectives and Functioning Principles

The proposed SMA-based device has been designed to be placed in series with a traditional steel tie-rod. In service conditions, the SMA device will be subjected to a tension force equal to the lateral thrusting force due to gravity loads. The main performance objective of the proposed SMA device is the limitation of the force variations in the steel tie-rod due to temperature changes in service conditions. An additional objective is the improvement of the seismic behavior of the tested structure under strong earthquakes.

The achievement of aforesaid performance objectives is strictly correlated to the superelastic properties of SMA (Ref 3, 13, 14). In service conditions, the thermal behavior of SMA results antagonistic compared to that of steel tie-rod. Indeed, as

This article is an invited paper selected from presentations at the International Conference on Shape Memory and Superelastic Technologies 2011, held November 6-9, 2011, in Hong Kong, China, and has been expanded from the original presentation.

Donatello Cardone and **Salvatore Sofia**, University of Basilicata, Viale dell'Ateneo Lucano 10, Potenza, Italy. Contact e-mails: donatello.cardone@unibas.it, donatello.c@tiscali.it, and salvatoresofia@libero.it.

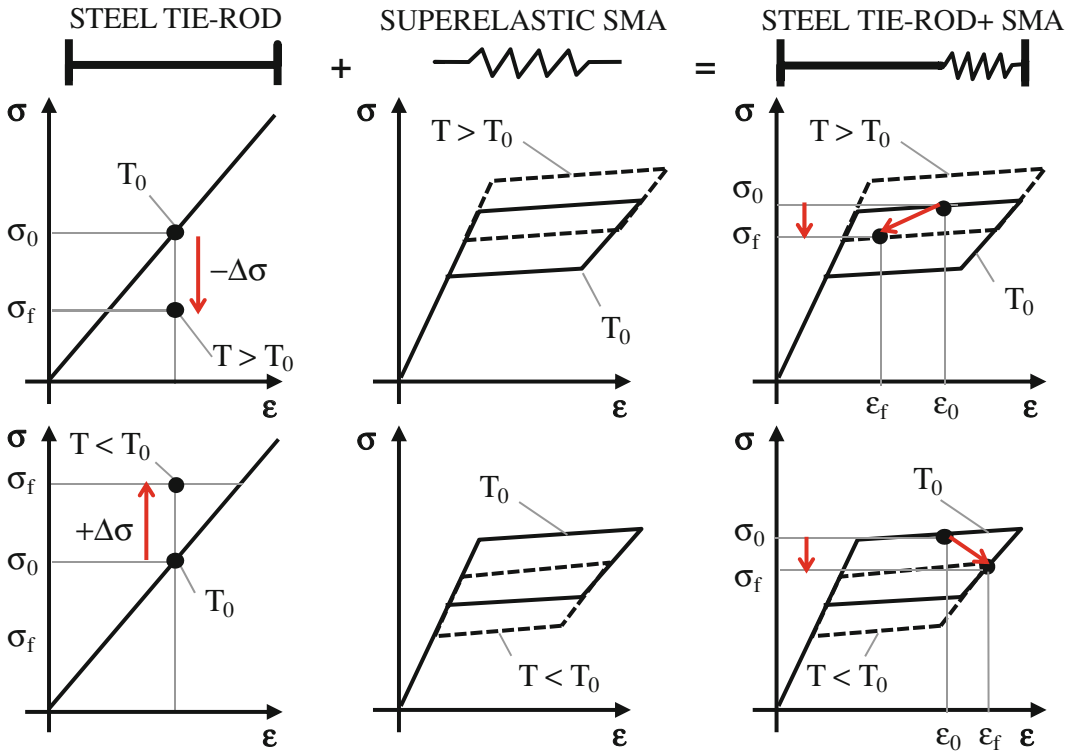

Fig. 1 Antagonistic thermal behavior between steel tie-rod and SMA superelastic device

soon as temperature increases (decreases) the tie-rod tends to elongate (shorten). The consequent reduction (increase) of axial force, however, is counterbalanced by the increase (reduction) of the stress levels in the SMA wires (see Fig. 1). From the seismic point of view, the improvement is related to the hysteretic energy dissipation capacity of pre-strained SMA wires, as well as to the excellent force control of the SMA wires during the martensitic transformation.

3. Evaluation of Thermal Behavior

The effectiveness of the proposed SMA-based device in service conditions has been evaluated through a numerical iterative procedure implemented in MATLAB (Ref 15), using an incremental formulation. The step-by-step procedure under consideration permits the evaluation of the thermal behavior of the system as a whole (steel tie-rod + SMA unit) subjected to a generic temperature history.

The thermomechanical behavior of SMA has been described with the phenomenological constitutive model developed by Brinson (Ref 16). The Brinson's model combines a phenomenological constitutive law, relating stress (σ), strain (ε), temperature (T), and martensite fraction (ξ), with a kinetic law that describes the evolution of the martensite fraction as a function of stress and temperature (transformation function). In this study, semi-empirical, rate-independent, cosine transformation functions, firstly proposed by Liang and Rogers (Ref 17), have been considered and implemented in the numerical procedure. The behavior of the structure (arch, vault, roof truss, etc.), under service condition, is governed by the following equilibrium and congruence equations:

$$A_{SMA} \cdot \sigma_{SMA} = A_{ROD} \cdot \sigma_{STEEL} \quad \text{(Eq 1)}$$

$$L_{SMA} \cdot \Delta\varepsilon_{SMA} = L_{ROD} \cdot \Delta\varepsilon_{STEEL} \quad \text{(Eq 2)}$$

in which A_{SMA} and A_{ROD} are the cross-section area of SMA device and steel tie-rod, respectively, L_{SMA} and L_{ROD} their corresponding lengths, σ_{SMA} and σ_{STEEL} the current stress levels in SMA wires and tie-rod, respectively, $\Delta\varepsilon_{SMA}$ and $\Delta\varepsilon_{STEEL}$ the associated thermally or stress-induced variations of strain. The variation of strain in the steel tie-rod can be expressed as:

$$\Delta\varepsilon_{STEEL} = \alpha \cdot \Delta T + (\Delta\sigma_{STEEL}/E_{STEEL}) \quad \text{(Eq 3)}$$

where α and E_{STEEL} are the thermal coefficient of expansion and the Young's modulus of the metallic material, respectively; ΔT and $\Delta\sigma_{STEEL}$ are the variations of air temperature and stress level in the steel tie-rod, respectively. The variation of strain in the SMA wires ($\Delta\varepsilon_{SMA}$) can be expressed as a function of $\Delta\sigma_{SMA}$ by inverting the constitutive laws of SMAs (Ref 16, 17). After that, Eq 1 and 2 provide the current value of the stress level in steel tie-rod and SMA wires. Once a given temperature-time history is assigned, a closed-form solution that describes the thermal behavior of the system in each instant of time can be obtained.

Figure 2 shows the thermal behavior of a steel tie-rod, with or without SMA device, as obtained from the numerical routine implemented in MATLAB. The tie-rod under consideration has 24 mm diameter cross section, 10 m length and it is supposed to work at approximately 180 MPa at 20 °C. The SMA device of Fig. 2 is composed of a proper number of SMA wires, having 70 mm length and 180 mm^2 overall cross-section area. The selected temperature-time history has been defined considering typical values of the maximum and minimum air temperature in Italy.

The SMA mechanical parameters that are required to explicit the numerical model have been obtained from a

number of tensile tests on superelastic wires, carried out at different temperatures ($T > M_s$) and pushed up to appearance of detwinned martensite (see Fig. 3). The aforesaid mechanical parameters include: (i) the four transformation temperatures in the stress-free state related to start and finish of the forward and inverse martensite transformation (M_s, M_f, A_s, and A_f), equal to −60, −49, −30.5 and −20 °C, respectively, in the case under consideration (see Fig. 3a); (ii) the maximum residual strain (ε_L) accumulated on complete stress-induced martensite transformation (see Fig. 4), approximately equal to 4.1% in the case under consideration; (iii) the slopes C_{AM} and C_{MA} of the transformation lines, equal to 6 and 6.1 MPa/°C, respectively (see Fig. 3a), and (iv) the Young's modules of SMA in the austenite (E_a) and martensite phase (E_m), equal to 60 and 15 GPa (see Fig. 4), respectively, in the case under consideration.

In Fig. 3(b), the experimental stress-strain relationships obtained from loading-unloading tension tests at different air temperatures (ranging from approximately 0 to 30 °C) are compared with the stress-strain curves provided by the adopted numerical model, using the experimental values of the SMA mechanical parameters listed before. The good accordance between experimental and numerical stress-strain diagrams confirms the accuracy of the selected SMA constitutive model, thus substantiating the numerical simulation presented in Fig. 2.

The structural system examined in Fig. 2 is assumed to undergo two thermal cycles characterized by a first heating from 20 to 40 °C, followed by cooling to 0 °C and then by further heating to 20 °C. As can be seen in Fig. 2, the total stress excursion experienced by the steel tie-rod is almost halved when the SMA unit is used. Considering the initial

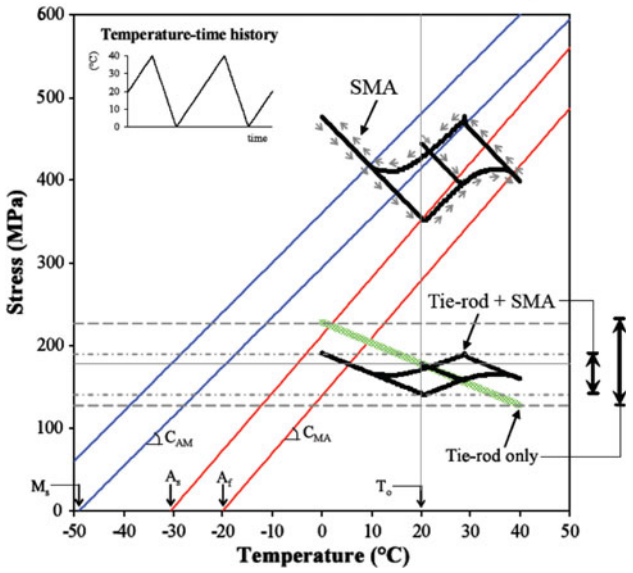

Fig. 2 Comparison between the thermal behavior of a steel tie-rod with and without SMA device based on the numerical simulation analysis

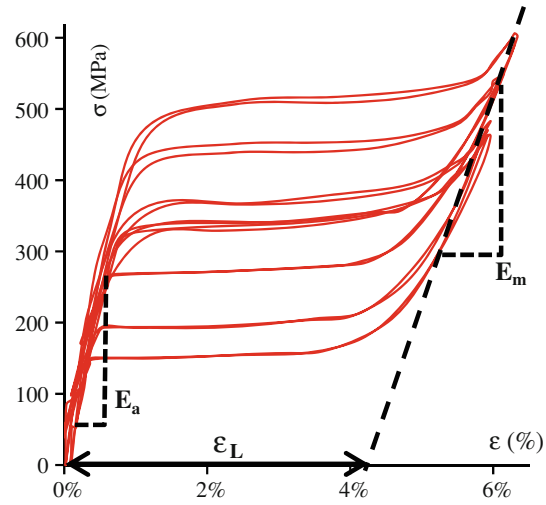

Fig. 4 Maximum residual strain (ε_L) and Young's modules of SMA in the austenite (E_a) and martensite (E_m) phase

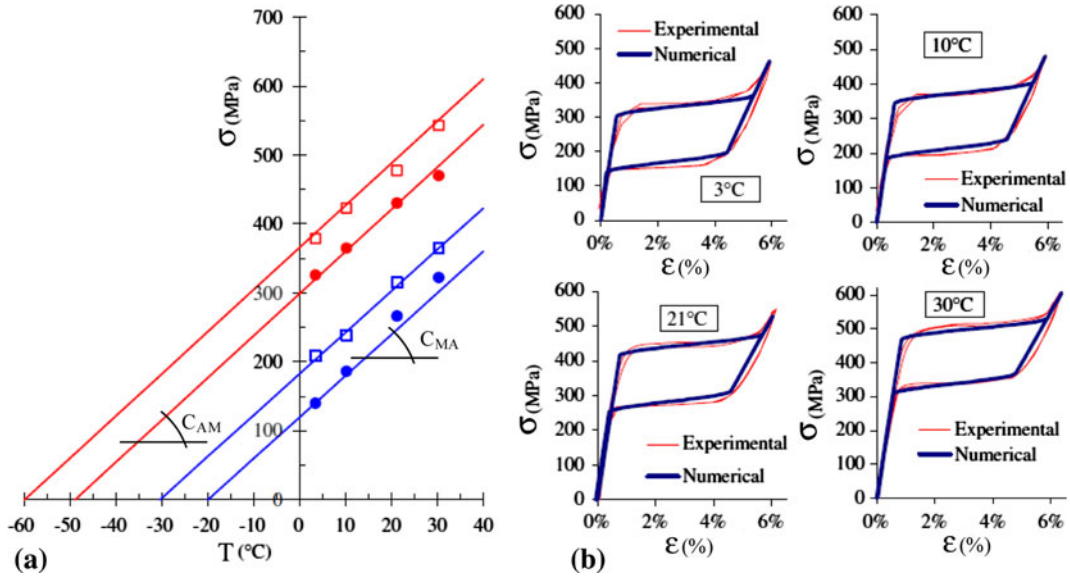

Fig. 3 Experimental results of loading-unloading tensile tests considered in the calibration of the SMA model: (a) critical transformation stresses as a function of temperature and (b) comparison between experimental and numerical stress-strain relationships at different air temperatures

stress level in the steel tie-rod at 20 °C, the maximum percent variation of stress is 29% without SMA unit, while it reduces to approximately 16% for the steel tie-rod with SMA unit. By examining the thermomechanical behavior of the SMA wires reported in Fig. 2, it is clear that the wider the transformation ranges (M_s-M_f and A_s-A_f) and the narrower the hysteretic range (M_s-A_s), the better the performances of the system.

Figure 5 shows the experimental apparatus set-up for thermal tests on tie-rod equipped with SMA device. It basically consists of (i) a steel testing rig, simulating the fixed restraint conditions imposed by arches and vaults, (ii) an Instron-Shenck dynamic actuator, able to apply 10 kN maximum force with ±125 mm stroke, simulating the steel tie-rod, (iii) a pre-strained SMA wire sample of 180 mm length, simulating the SMA device, and (iii) a thermal room, working in a temperature range from −30 to +80 °C. The test apparatus of Fig. 5 has been purposely designed to reproduce the work conditions that a metallic tie-rod with SMA device would experience when inserted inside an arch or a vault.

The presence of the steel tie-rod in the experimental tests is simulated with the actuator that is driven by special software which controls the SMA displacement according to the following algorithm:

$$d = d_0 - \alpha \cdot L_{ROD} \cdot (T - T_0) - \frac{L_{ROD}}{E \cdot A_{ROD}} \cdot (F - F_0) \qquad \text{(Eq 4)}$$

where d_0, T_0, and F_0 are the imposed initial displacement, force, and air temperature, respectively, L_{ROD} and A_{ROD} are the length and cross-section area of the steel tie-rod, E and α are the Young's modulus and thermal coefficient of expansion of steel. The displacements applied by the actuator to the SMA wires, therefore, take into account both the elastic deformation and the thermal expansion of the steel tie-rod.

Figures 6 and 7 show the results of two typical tests carried out with the experimental apparatus of Fig. 5. In both the cases, the following assumptions have been made for the steel tie-rod: L_{ROD} = 10 m, $\alpha = 1.2 \times 10^{-5}$ °C^{-1}, E = 210 GPa, and $\sigma_0 = F_0/A_{ROD}$ = 100 MPa. The SMA unit consists of one 1.84 mm diameter SMA wire with 180 mm free length.

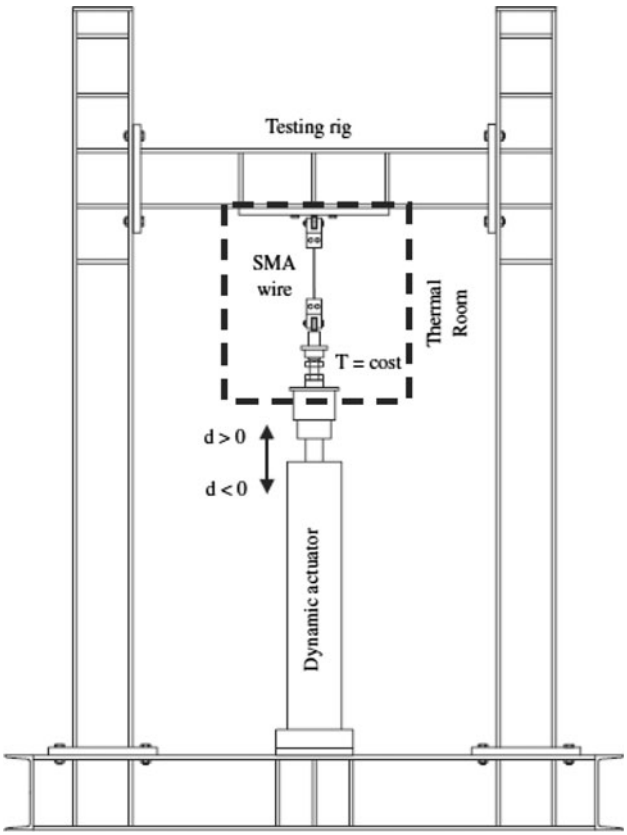

Fig. 5 Experimental apparatus for thermal tests under displacement control

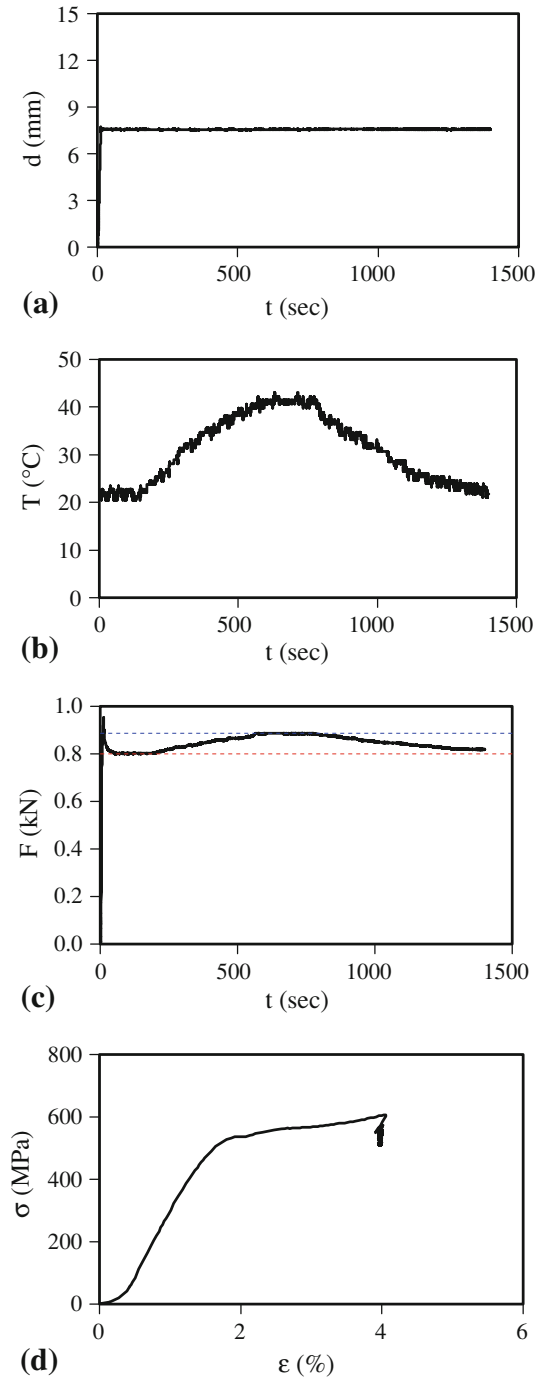

Fig. 6 Experimental behavior of steel rod + SMA device during heating from 20 to 40 °C followed by cooling to 20 °C: (a) displacement, (b) air temperature, and (c) force-time histories of the entire system. (d) Stress-strain behavior of SMA wires

In the first test, a displacement of about 7.5 mm (corresponding to a pre-strain of about 4% in the SMA wire sample) is applied and maintained constant during the test (see Fig. 6a). The air temperature is first increased from 20 to 40 °C and then decreased again to 20 °C (see Fig. 6b). In the second test, a displacement of 9 mm (corresponding to about 5% pre-strain in the SMA wire sample) is applied and maintained constant during the test (see Fig. 7a). The air temperature is first decreased from 20 °C to approximately 0 °C and then increased again to 20 °C (see Fig. 7b). During the tests, the force acting in the system is constantly monitored (see Fig. 6c, 7c). The examination of the force-time histories recorded during the tests (see Fig. 6c, 7c) points out a percent variation of force of the order of 10-12%, to be compared with that experienced by the tie-rod without SMA device ($\Delta F/F_0 = \alpha E_{STEEL} A_{ROD} \Delta T/\sigma_0$) under the same experimental conditions, of the order of 50% in both the cases.

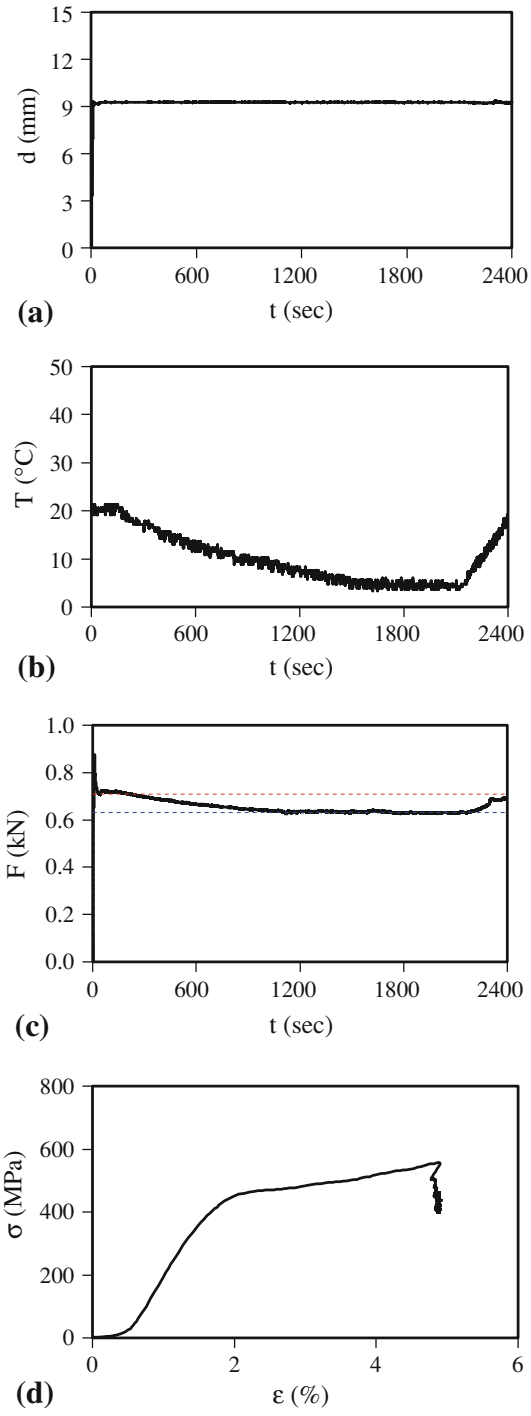

Fig. 7 Experimental behavior of steel rod + SMA device during cooling from 20 to 0 °C followed by heating to 20 °C: (a) displacement, (b) air temperature, and (c) force-time histories of the entire system. (d) Stress-strain behavior of SMA wires

4. Shaking Table Tests

The proposed SMA device has been designed to reach a number of performance objectives under seismic conditions: (i) to avoid yielding and buckling in the steel tie-rod, (ii) to re-center the structure in its initial configuration at the end of seismic displacements, (iii) to control the maximum displacement under earthquakes with seismic intensity higher than the design level. The scope of the experimental seismic tests was to demonstrate that the aforesaid objectives are fully achieved with proposed SMA device.

4.1 Specimens

The experimental model (Fig. 8) is a 1:4-scale timber roof truss model characterized by a static scheme of three-hinges arch with 1.5 m span and 0.5 m rise. The experimental model consists of two wooden layers, with plan dimensions of 0.95 m × 1 m and 50 mm thickness, inclined at 35° with respect to the horizontal line and supported by two wooden beams with 0.1 m × 0.1 m cross section. The wooden layers are connected at the ridge through a cylindrical steel hinge, free to rotate due to insertion of a number of polytetrafluoroethylene (PTFE) washers between the steel bar and the wood holes.

The model is placed on the earthquake platform through two bearing devices (Fig. 8): one sliding in the seismic direction while the other rigidly fixed to the table. The absolute displacement of the sliding bearing corresponds to the relative movements between the walls supporting the roof (or the piers of an arch/vault) in a real structure. The sliding bearing at the base of the model is realized with four 1 mm diameter circular PTFE pads with recesses and a 2 mm thickness stainless steel shim. Based on the contact pressure generated in the PTFE pads (equal to about 5 MPa) a friction coefficient of the order of 5% was expected between lubricated stainless steel and PTFE interfaces (Ref 18). The two bearing devices have been

Fig. 8 Experimental model ready to be tested

connected by means of a steel bar with 4 mm diameter, 900 mm length, and approximately 3 kN tensile strength. The steel bar was designed to absorb the horizontal thrust due to gravity loads working at approximately 50% its ultimate strength.

Additional masses were put on each layer of the model, to account for the non-structural dead loads, a fraction (1/3) of live loads and the increase of mass in the model due to the mass similitude scaling. To this end, 36 steel disks, 10 kg each, were put on each layer of the model.

The SMA device employed in the tests (Fig. 9) was realized using a 1 mm diameter superelastic Ni-Ti SMA wire. Ni-Ti SMA have been preferred to other types of SMA (e.g., Cu-based SMA) due to its higher energy dissipation capacity, larger superelastic strain range and better fatigue resistance to large strain cycles. In the test configuration, the SMA wire was wrapped around two redances and fastened by means of a couple of clamps. A total of 2.5 wire loops were realized, in order to limit the maximum force transmitted by the SMA device below the yield force of the steel tie-rod. The free length of the SMA wires, measured as the distance between the two clamps, was set equal to 150 mm, corresponding to a total length of the device equal to 210 mm. Between one test sequence and another, the SMA wire was replaced with a new one. During this operation the sliding bearing of the model was bolted to the earthquake platform by means of a couple of rigid steel plates.

4.2 Test Set-up

The test apparatus for shaking table tests consists of a single-degree-of-freedom earthquake platform with 1940 × 950 mm dimensions and 1 ton load capacity. The earthquake platform is driven by a dynamic Instron-Schenk actuator fixed to an external rigid metal frame and powered by a hydraulic control unit with approximately 160 L/min capacity. The actuator is characterized by a maximum force of 40 kN and maximum stroke of ±125 mm. The sensor set-up for the acquisition of the seismic response of the experimental model includes (Fig. 10): (i) two LVDT's with ±50 mm working range, measuring the horizontal displacements of the sliding bearing at the base of the model, (ii) one LVDT with ±50 mm working range, measuring the relative displacements between the ends of the SMA wire loops, (iii) one LVDT with ±25 mm working range, measuring the vertical displacements of the hinge placed on the roof, (iv) two ±2 g servoaccelerometers, measuring the horizontal accelerations of earthquake platform and wooden layer, respectively, (v) one inclinometer with ±10° operational range, measuring the rotations of a layer, and (vi) a double-effect load cell with ±5 kN working range, measuring the tension force in the tie-rod.

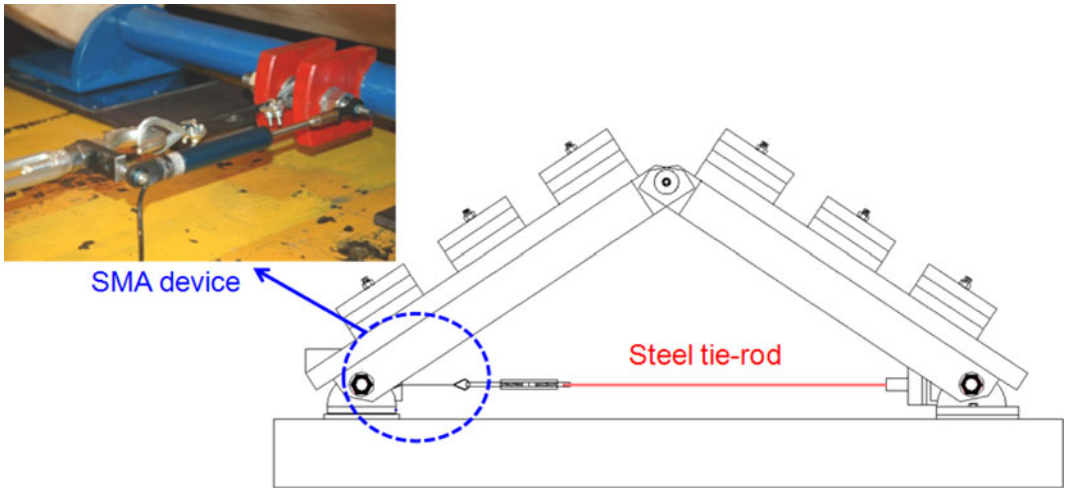

Fig. 9 Close-up view of the SMA system

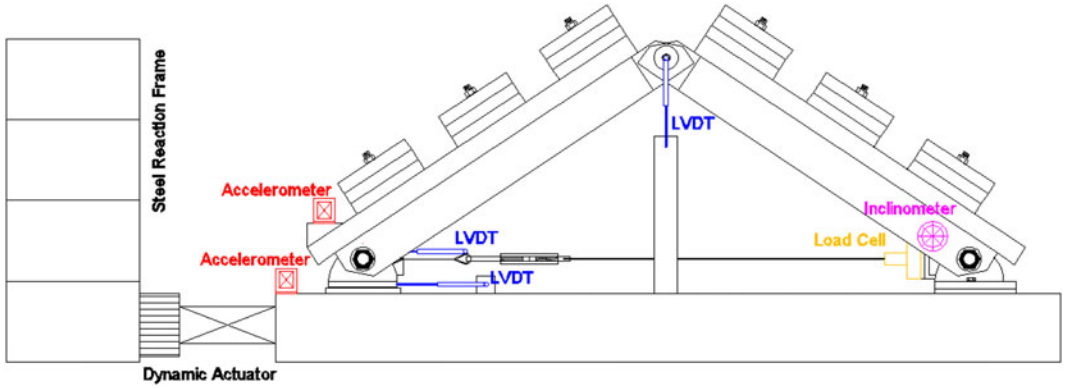

Fig. 10 Schematic layout of experimental model and sensor set-up

4.3 Experimental Program

The main purpose of the experimental program was to assess the effectiveness of the SMA-based device in improving the seismic response of the structural model, by overcoming the main limitations of the traditional metallic tie-rods. The complete program of tests includes a total of 34 shaking table tests, the first 18 on the model equipped with SMA-based unit and the subsequent 16 on the model with steel tie-rod only.

Two artificial accelerograms, strictly compatible with the Eurocode 8 (Ref 19) elastic response spectrum for soil type B, and two natural records (i.e., the WE component of the L'Aquila station (4.9 km epicentral distance) of the L'Aquila mainshock (06/04/2009) earthquake (Magnitude 6.3), and the NS component of the Tolmezzo station (21.7 km epicentral distance) of the Friuli mainshock (06/05/1976) earthquake (Magnitude 6.4)) have been selected as input signal of the earthquake platform (Fig. 11).

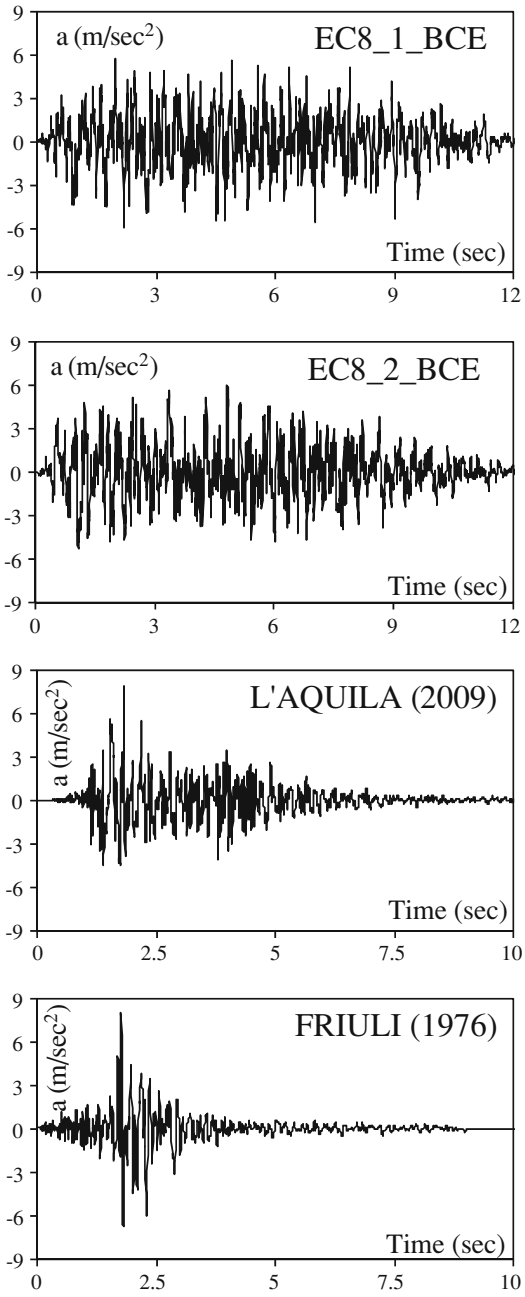

Fig. 11 Input acceleration profiles used for experimental seismic tests

The input signals have been scaled in time by a factor equal to the square root of the scale of the model in accordance with the principles of the theory of model scaling. The PGA of the input signals has been progressively increased during the tests, up to the operative limits of the SMA unit or the occurrence of extensive damage in the metallic tie-rod. The tests at the maximum seismic intensities (0.6 g for the artificial accelerograms and 0.8 g for the natural records) have been repeated within a single run test sequence. At the end of each test sequence (same structural configuration and same seismic input), SMA wires and steel bar have been replaced with new ones.

5. Experimental Results

Figure 12 compares the experimental cyclic behavior of the tie-rod with and without SMA device, recorded during the tests with the artificial accelerograms at 0.6 g (Fig. 12a, b) and with the L'Aquila and the Friuli natural records at 0.8 g (Fig. 12c, d). As can be seen, the cyclic behavior of the tie-rod with SMA device results compatible with the design strain amplitude of SMA, which is typically assumed equal to that corresponding to the end of the martensitic transformation (about 9% in the case under consideration). Indeed, the maximum strain amplitude attained during the tests considered in Fig. 12 ranges between 9 and 11%. Similar considerations can be done in terms of force transmitted by the SMA unit to the steel bar, which ranges between 2.4 and 2.7 kN, thus resulting fully compatible with the yielding force of the steel bar, equal to approximately 3 kN.

Figure 13 compares the displacement-time histories of the horizontal displacement of the sliding bearings recorded during the tests with the artificial accelerograms at 0.6 g (Fig. 13a, b) and with the L'Aquila and Friuli natural records at 0.8 g (Fig. 13c, d).

The use of the SMA device results in a significant increase of the deformability of the structure, well pointed by the increase of its equivalent period of vibration, from about 0.12 s (tie-rod without SMA unit) to about 0.2 s (tie-rod with SMA unit). The aforesaid values of the equivalent period of vibration of the testing model have been evaluated based on the secant stiffness of the tie-rod with and without SMA at the maximum displacement amplitudes attained during the tests. This should imply larger horizontal displacements in presence of SMA unit.

Nevertheless, the maximum displacements of the structure with and without SMA unit are still comparable (24 versus 19 mm for the artificial accelerogram n. 1 (Fig. 13a) and 15 versus 22 mm for the artificial accelerogram n. 2 (Fig. 13b), due to the significant displacement offset consequent to the yielding of steel bar. The cyclic behavior of the system equipped with the SMA unit turns out to be perfectly re-centering. On the contrary, the tie-rod without SMA unit underwent extensive plastic deformations, with large residual displacements at the end of the earthquake, which are of the order of 21 and 8 mm for the accelerograms n. 1 and n. 2, respectively, corresponding to residual deformation in the steel bar of the order of 2.4 and 0.9%, respectively. In this case, the tie-rod must be immediately replaced in order to avoid the collapse of the steel bar due to possible aftershocks. No instability phenomena have been registered during the tests on

the structure with SMA unit, while the buckling of the steel bar has been observed occasionally during the tests on the structure without SMA unit (Fig. 12a, b).

Figure 14 shows the Frequency S-Transform Functions (Ref 20, 21) derived from the acceleration-time histories of the model with SMA unit, recorded during the test at 0.6 g with the artificial accelerogram n. 1 (Fig. 14a) and during the test at 0.8 g with the L'Aquila natural record (Fig. 14b). As can be seen, the fundamental frequency of vibration of the structure with SMA unit varies during the seismic excitation, decreasing from approximately 6-7 Hz to 3-4 Hz, while increasing the amplitude of seismic vibrations. At the end of the earthquake, however, the frequency of vibration reaches again the same initial value, as a result of the strong re-centering behavior of the SMA device. Also the frequency of vibration of the structure without SMA device (Fig. 14c) changes continuously during the seismic excitation, decreasing from approximately 10-11 Hz to 5-6 Hz, while increasing the amplitude of seismic vibrations. During the coda stage of the test, however, the frequency of vibration stabilizes around 8 Hz, as a consequence of steel yielding.

The maximum horizontal displacement registered during the seismic tests on the model with SMA unit resulted of the order of 25 mm, corresponding to a full-scale displacement of the top of the walls that sustain the roof of the order of 50 mm.

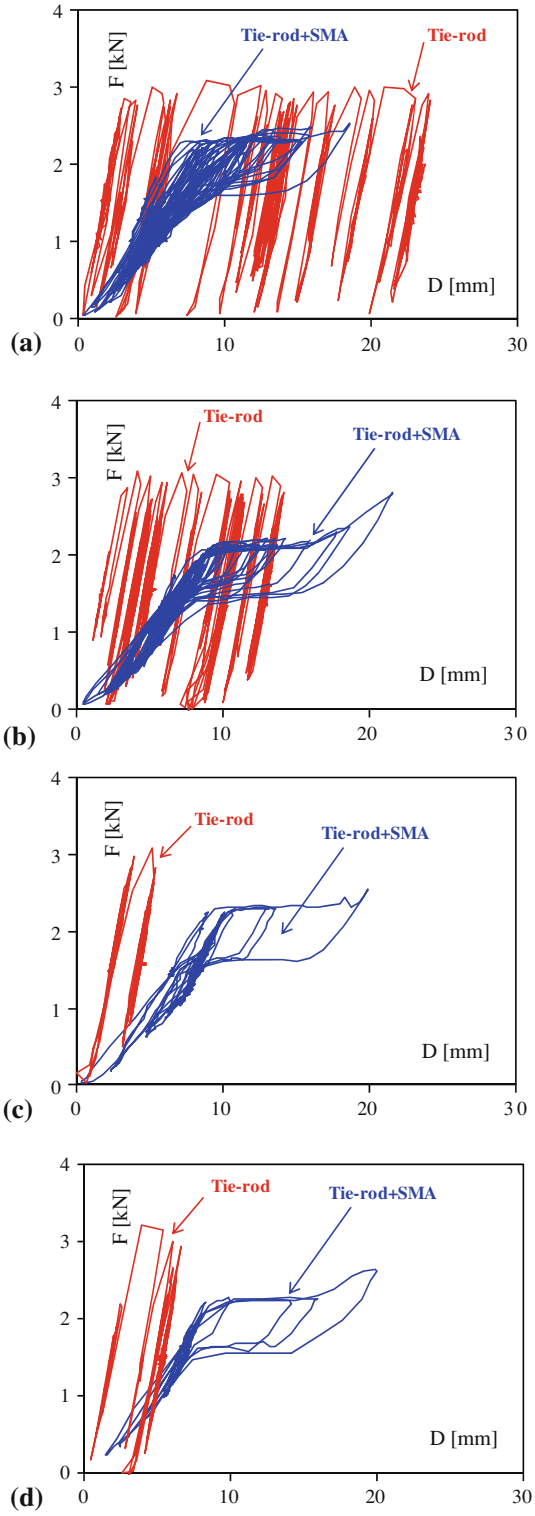

Fig. 12 Comparison between force-displacement cyclic behaviors of tie-rod with and without SMA for (a) artificial accelerogram n. 1 at 0.6 g, (b) artificial accelerogram n. 2 at 0.6 g, (c) L'Aquila record at 0.8 g, and (d) Friuli record at 0.8 g

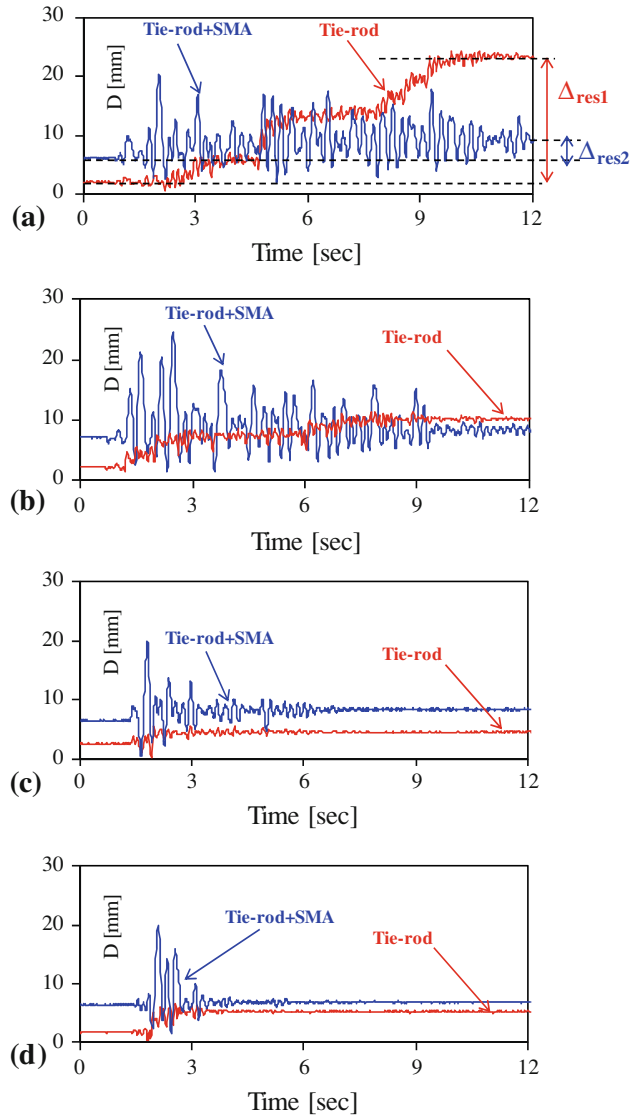

Fig. 13 Comparison between horizontal displacement-time histories of tie-rod with and without SMA for (a) artificial accelerogram n. 1 at 0.6 g, (b) artificial accelerogram n. 2 at 0.6 g, (c) L'Aquila record at 0.8 g, and (d) Friuli record at 0.8 g

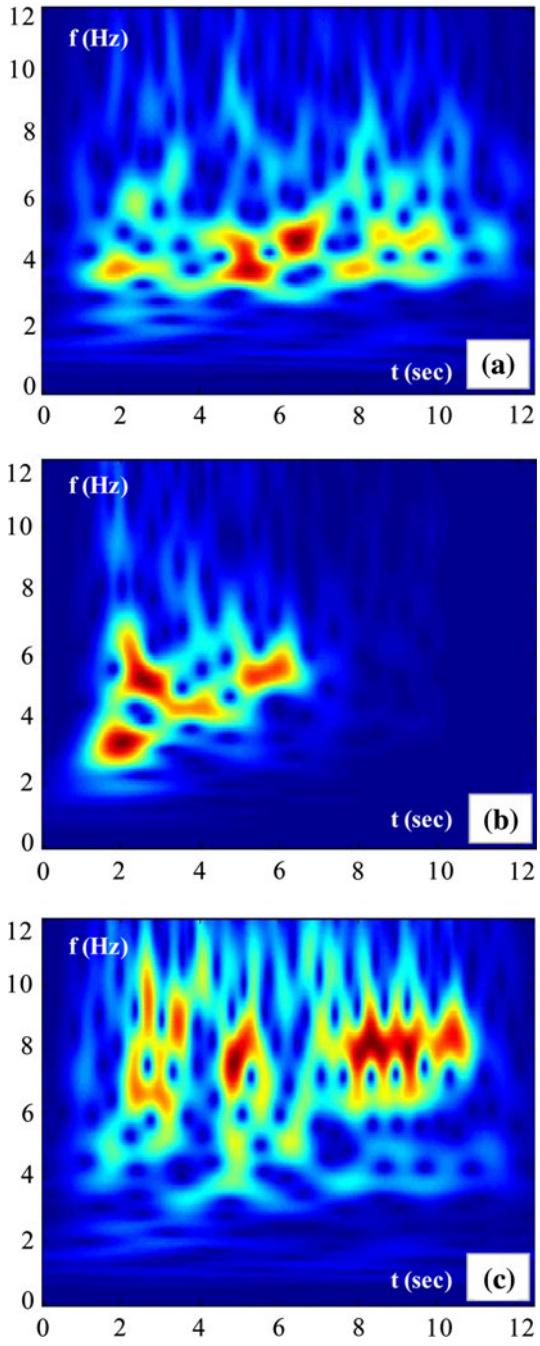

Fig. 14 S-Transform Functions derived from the acceleration response of the model (a, b) with and (c) without SMA unit

The compatibility of the maximum displacement can be checked by examining the out-of-plane collapse mechanism of masonry walls. To this end, reference to the nonlinear cinematic approach proposed in the Italian seismic code (Ref 22) can be made. According to this approach, masonry walls with typical dimension and mechanical characteristics exhibit a displacement capacity approximately two times bigger than the maximum displacement said before. This proves that the seismic response of the model with SMA unit, observed during the experimental tests carried out in this study, is compatible with the out-of-plane resistance of typical masonry walls.

6. Conclusions

A prototype device based on Ni-Ti SMAs for the improvement of the service and seismic performances of metallic tie-rods for historical buildings has been presented.

A number of preliminary experimental and numerical studies have been carried out, in order to investigate the thermal behavior of the proposed SMA-based device. The results of these preliminary studies prove the effectiveness of the proposed SMA device in limiting force changes in metallic tie-rods due to air temperature variations. Further improvements may be obtained using SMAs with a less hysteretic cyclic behavior, such as that of the Cu-based SMAs.

Extensive shaking table tests have been also carried out, to investigate the behavior of the proposed SMA-based device under strong earthquakes. The results of shaking table tests clearly prove the effectiveness of the proposed SMA device in improving the seismic response of arches, vaults, and roof trusses equipped with traditional metallic tie-rods. This can be ascribed to the longer equivalent period of vibration, higher energy dissipation capacity, and better control of force guaranteed by the use of the proposed SMA device.

Considering the displacement levels associated to the out-of-plane collapse of the supporting walls, the PGA corresponding to the attainment of the ultimate strength of the metallic tie-rod can be further increased by increasing the length of the SMA wires. Excessive lengths, however, could be at the detriment of the performances of the system (tie-rod + SMA) in service conditions (thermal behavior) that in many cases appears to be the main design objective of the proposed SMA device.

Obviously, the design shall be made considering the response of the system both under service conditions (thermal behavior) and under ultimate conditions (seismic behavior). As a consequence, the optimal solution should be derived based on preliminary considerations on the seismicity of the area and its environmental conditions: an optimal seismic behavior of the SMA device shall be pursued for structures in high seismicity regions where moderate temperature changes are expected; vice versa an optimal thermal behavior of the SMA device shall be pursued for structures in low seismicity regions where considerable temperature changes are expected.

Acknowledgments

This work has been carried out within a research contract with CETMA (Center Planning, Design and Technology of Materials) of Brindisi (Italy). The authors are also grateful to Domenico Nigro (University of Basilicata) for his valuable help in setting up the testing apparatus and executing the experimental tests.

References

1. M. Dolce, D. Cardone, and R. Marnetto, Implementation and Testing of Passive Control Devices Based on Shape Memory Alloys, *Earthq. Eng. Struct. Dyn.*, 2000, **29**(7), p 945–968
2. M. Dolce and D. Cardone, Mechanical Behaviour of Shape Memory Alloys for Seismic Applications—1. Martensite and Austenite NiTi Bars Subjected to Torsion, *Int. J. Mech. Sci.*, 2001, **43**(11), p 2631–2656
3. M. Dolce and D. Cardone, Mechanical Behavior of SMA Elements for Seismic Applications—Part 2. Austenite NiTi Wires Subjected to Tension, *Int. J. Mech. Sci.*, 2001, **43**(11), p 2657–2677

4. D. Cardone, M. Dolce, F.C. Ponzo et al., Experimental Behaviour of R/C Frames Retrofitted with Dissipating and Re-centring Braces, *J. Earthq. Eng.*, 2004, **8**(3), p 361–396
5. A. Jalali, D. Cardone, and P. Narjabadifam, Smart Restorable Sliding Base Isolation System, *Bull. Earthq. Eng.*, 2011, **9**(2), p 657–673
6. D. Cardone, P. Narjabadifam, and D. Nigro, Shaking Table Tests of the Smart Restorable Sliding Base Isolation System (SRSBIS), *J. Earthq. Eng.*, 2011, **15**(8), p 1157–1177
7. G. Attanasi and F. Auricchio, Innovative Superelastic Isolation Device, *J. Earthq. Eng.*, 2011, **15**, p 72–89
8. G. Attanasi, F. Auricchio, and G.L. Fenves, Feasibility Assessment of an Innovative Isolation Bearing System with Shape Memory, *J. Earthq. Eng.*, 2009, **13**, p 18–39
9. J. McCormick, R. DesRoches, D. Fugazza et al., Seismic Assessment of Concentrically Braced Steel Frames with Shape Memory Alloy Braces, *J. Struct. Eng.*, 2007, **133**(6), p 862–870
10. B. Andrawes and R. DesRoches, Comparison Between Shape Memory Alloy Seismic Restrainers and Other Bridge Retrofit Devices, *J. Bridge Eng.*, 2007, **12**(6), p 700–709
11. B. Andrawes and R. DesRoches, Unseating Prevention for Multiple Frame Bridges Using Superelastic Devices, *Smart Mater. Struct.*, 2005, **14**(3), p 60–67
12. R. DesRoches and M. Delemont, Seismic Retrofit of Simply Supported Bridges Using Shape Memory Alloys, *Eng. Struct.*, 2002, **24**(3), p 325–332
13. D. Cardone and M. Dolce, SMA-Based Tension Control Block for Metallic Tie-rods, *Int. J. Mech. Sci.*, 2008, **51**, p 159–165
14. H. Funakubo, *Shape Memory Alloys*, Gordon & Breach Science Publishers, New York, 1995
15. MathWorks, *MATLAB 7.5-release 2007b*, 2007
16. L.C. Brinson, One-dimensional Constitutive Behavior of Shape Memory Alloys: Thermomechanical Derivation with Non-constant Material Functions and Redefined Martensite Internal Variable, *J. Intell. Mater. Syst. Struct.*, 1993, **4**, p 229–242
17. C. Liang and C.A. Rogers, A Multi-dimensional Constitutive Model for Shape Memory Alloys, *J. Eng. Math.*, 1992, **26**, p 429–443
18. M. Dolce, D. Cardone, and F. Croatto, Frictional Behavior of Steel-PTFE Interfaces for Seismic Isolation, *Bull. Earthq. Eng.*, 2005, **3**(1), p 75–99
19. CEN (Comité Europeen de Normalization), *Eurocode 8: Design of Structures for Earthquake Resistance—Part 1: General Rules, Seismic Actions and Rules for Buildings*, Brussels, 1998
20. R. Ditommaso, M. Mucciarelli, F.C. Ponzo, S-Transform Based Filter Applied to the Analysis of Non-linear Dynamic Behavior of Soil and Buildings, *14th ECEE*, Ohrid, Republic of Macedonia, 2010
21. R. Stockwell, L. Mansinha, and R.P. Lowe, Localization of the Complex Spectrum: The S Transform, *IEE Trans. Signal Process*, 1996, **44**, p 998–1001
22. Ministero delle Infrastrutture e dei Trasporti, *D.M. 14 gennaio 2008—Norme tecniche per le costruzioni*, 2008 (in Italian)